Published in final edited form as:
Vision Res. 2015 February ; 107: 58–66. doi:10.1016/j.visres.2014.12.001.

Temporal characteristics of melanopsin inputs to the human pupil light reflex

Daniel S. Joyce[1], **Beatrix Feigl**[1,2], **Dingcai Cao**[3], and **Andrew J. Zele**[1,*]

[1]Visual Science and Medical Retina Laboratories, Institute of Health and Biomedical Innovation, Queensland University of Technology, Brisbane, Australia

[2]Queensland Eye Institute, Brisbane, Australia

[3]Department of Ophthalmology and Visual Sciences, University of Illinois at Chicago, USA

Abstract

Rods, cones and melanopsin containing intrinsically photosensitive Retinal Ganglion Cells (ipRGCs) operate in concert to regulate pupil diameter. The temporal properties of intrinsic ipRGC signalling are distinct to those of rods and cones, including longer latencies and sustained signalling after light offset. We examined whether the melanopsin mediated post-illumination pupil response (PIPR) and pupil constriction were dependent upon the inter-stimulus interval (ISI) between successive light pulses and the temporal frequency of sinusoidal light stimuli. Melanopsin excitation was altered by variation of stimulus wavelength (464 nm and 638 nm lights) and irradiance (11.4 and 15.2 log photons.cm^{-2}.s^{-1}). We found that 6s PIPR amplitude was independent of ISI and temporal frequency for all melanopsin excitation levels, indicating complete summation. In contrast to the PIPR, the maximum pupil constriction increased with increasing ISI with high and low melanopsin excitation, but time to minimum diameter was slower with high melanopsin excitation only. This melanopsin response to briefly presented pulses (16 and 100 ms) slows the temporal response of the maximum pupil constriction. We also demonstrate that high melanopsin excitation attenuates the phasic peak-trough pupil amplitude compared to conditions with low melanopsin excitation, indicating an interaction between inner and outer retinal inputs to the pupil light reflex. We infer that outer retina summation is important for rapidly controlling pupil diameter in response to short timescale fluctuations in illumination and may occur at two potential sites, one that is presynaptic to extrinsic photoreceptor input to ipRGCs, or another within the pupil control pathway if ipRGCs have differential temporal tuning to extrinsic and intrinsic signalling.

*Corresponding Author. Address: Institute of Health and Biomedical Innovation, 60 Musk Avenue, Kelvin Grove, Queensland 4059, Australia., Phone: +61 7 31386151, andrew.zele@qut.edu.au.

Keywords

intrinsically photosensitive retinal ganglion cells (ipRGC); melanopsin; post-illumination pupil response (PIPR); pupil light reflex; summation

1. Introduction

Intrinsically photosensitive Retinal Ganglion Cells (ipRGCs) have two primary functions; the non-image forming transduction of light via projections to the suprachiasmatic nucleus (SCN) for circadian photoentrainment (Berson, Dunn, & Takao, 2002; Do & Yau, 2010; Gooley, Lu, Fischer, & Saper, 2003; Güler et al., 2008), and the regulation of pupil diameter through projections to the olivary pretectal nucleus (OPN) (Hattar et al., 2006). These two functions operate within different temporal scales; ipRGCs have long term signalling capabilities of at least 10 hours in duration (Wong, 2012) for circadian photoentrainment to the solar day, while pupil constriction has a similar critical duration to that of image-forming visual processes (Webster, 1969).

The ipRGCs in the inner retina signal light information via the intrinsic photopigment melanopsin (Hattar, Liao, Takao, Berson, & Yau, 2002; Lucas, Douglas, & Foster, 2001; Provencio, Rollag, & Castrucci, 2002) and response onset varies from ~1 minute at ipRGC threshold to several hundred milliseconds at saturating irradiances (Berson et al., 2002), with a time to peak spiking at ~3 s (Dacey et al., 2005). The intrinsic melanopsin contribution can be observed directly in primates and humans as a sustained pupil constriction after light offset (Gamlin et al., 2007); as the spectral sensitivity of this human post-illumination pupil response (PIPR) closely matches that of the melanopsin photopigment when measured with 10 s aperiodic stimuli (Gamlin et al., 2007; Markwell, Feigl, & Zele, 2010). IpRGCs also receive extrinsic inputs from outer retinal rods and cones (Dacey et al., 2005; Lucas et al., 2003; Schmidt & Kofuji, 2010) and this combination of intrinsic and extrinsic signalling regulates pupil diameter (Barrionuevo et al., 2014; Gamlin et al., 2007; Markwell et al., 2010; McDougal & Gamlin, 2010; Tsujimura, Ukai, Ohama, Nuruki, & Yunokuchi, 2010).

It is not well understood how inner and outer retinal inputs that have different temporal response properties are combined to modulate pupil diameter. Temporal summation is a fundamental image-forming process that balances visual sensitivity with temporal resolution to optimise visual performance, but little is known about the summation properties of melanopsin inputs to the non-imaging process of pupil regulation, namely the amplitude of constriction and PIPR. For image-forming vision, stimulus irradiance and duration are reciprocal for durations between ~75 to ~100 ms under dark adapted conditions, with a similar critical duration required to achieve a criterion pupil constriction (Webster, 1969). The critical duration of the PIPR is yet to be established, although it is likely to be longer given the extended latent period of ipRGCs (Berson et al., 2002). In humans, the maintained pupil constriction during stimulus presentation of narrow-band light pulses less than 10 s duration is predominantly driven by outer retinal signalling (rods; and to a lesser degree, cones) (McDougal & Gamlin, 2010), mediated extrinsically via the ipRGC pathway to the OPN (McDougal & Gamlin, 2008). The outer retina dominated pupil constriction amplitude measured under conditions not optimised to study the role of melanopsin signalling shows

summation over inter-stimulus intervals (ISI) of approximately 600 ms (Baker, 1963). In Experiment 1 we determined the summation properties of the pupil constriction amplitude and the melanopsin mediated PIPR under high and low melanopsin excitations in response to two aperiodic light pulses separated in time.

The phasic pupil response to sinusoidal light stimulation (Barrionuevo et al., 2014; Clarke, Zhang, & Gamlin, 2003; Stark & Baker, 1959; Stark & Sherman, 1957) is dominated by outer retinal rod and cone photoreceptor inputs with an augmented melanopsin contribution with increasing light level (Barrionuevo et al., 2014). In Experiment 2 we determined the effect of periodic stimulation with high and low melanopsin excitations on the PIPR amplitude and phasic pupil response, to identify a signature interaction between inner and outer retinal inputs.

2. Materials and Methods

2.1 Apparatus

Light stimuli were generated using a custom-built optical system with the design based on an extended Maxwellian view optical system (Beer, MacLeod, & Miller, 2005; Kankipati, Girkin, & Gamlin, 2010). Light generated by 5 mm LEDs (blue appearing short wavelength: λ_{max} = 464 nm, 19 nm half-bandwidth; red appearing long wavelength: λ_{max} = 638 nm, 15 nm half-bandwidth) was imaged in the plane of the right pupil via two Fresnel lenses (100 mm diameter, 127 mm and 70 mm focal lengths; Edmund Optics, Singapore) and a 5° light shaping diffuser (Physical Optics Corp., California USA). This generated a 35.6° diameter stimulus light and its corresponding ~31.8 mm diameter retinal image. The consensual pupil response of the left eye was recorded under infrared LED illumination (λ_{max} = 851 nm) with a Pixelink camera (PL-B741 FireWire; 640 × 480 pixels; 60 frames.s^{-1}) through a telecentric lens (Computar 2/3″ 55 mm and 2× Extender C-Mount). A chin rest, temple bars and a head restraint maintained alignment.

All electronics were supplied from stabilised power supplies and stimuli irradiances confirmed with a calibrated radiometer (International Light Technologies IL1700, USA). The temporal profiles of all stimuli were confirmed with a high resolution digital acquisition device (ADI Instruments, USA) connected to a silicon cell. Data were recorded at 60 Hz and digitally filtered using a lowpass 6^{th} order Butterworth IIR with a 5 Hz cut-off frequency. The filter was confirmed to introduce no phase shifting of the data, and missing data points due to blinks were linearly interpolated. Custom software coded in Matlab (version 7.12.0, Mathworks, USA) controlled stimulus presentation, pupil recording and analysis. Details are given elsewhere (Feigl, Mattes, Thomas, & Zele, 2011; Zele, Feigl, Smith, & Markwell, 2011).

2.2 Experimental Paradigms

Blue (B, 464 nm) or red (R, 638 nm) appearing narrow-band stimuli at low (L, 11.4 log photons.cm^{-2}.s^{-1}) or high (H, 15.2 log photons.cm^{-2}.s^{-1}) irradiance were used. Table 1 specifies the relative photoreceptor excitation (α-opic lux) for each irradiance/wavelength combination (Lucas et al., 2014). Conditions are specified in terms of melanopsin excitation, with M+ and M− for high or low melanopsin excitation and the subscripts indicating the

wavelength (B for the blue LED and R for the red LED) and irradiance level (L for low irradiance and H for high irradiance). Condition M^{+}_{BH} (4453 melanopic lux) has a ~1600-fold greater melanopsin excitation than the three other conditions (M^{-}_{BL}, M^{-}_{RH}, M^{-}_{RL}; ≤ 2.78 melanopic lux). Condition M^{+}_{BH} also produces higher outer retina photoreceptor excitations (L-, M- and S-cone and rods) than the M^{-} conditions. Note that Table 1 specifies the relative photoreceptor excitations given photoreceptor spectral sensitivities, the spectral properties of the stimulus and ocular prereceptoral attenuation; with no indication of their effect on the pupil. Individual photoreceptor contributions to the pupil control pathway cannot be inferred based on stimulus α-opic lux alone, being further dependent on the spatial and temporal properties of the stimulus and the photoreceptor inputs to the pupillary control pathway under the measured conditions; the roles of many of these factors are still to be determined. Furthermore, the generalizability of one melanopic lux metric to the activity of all five subtypes (M1–M5) has not been established, nor has the individual contributions of these subtypes to the human pupil control pathway. A sustained PIPR compared to baseline confirms melanopsin pathway activation (for review, see Feigl & Zele, 2014), as the human PIPR has the same spectral response as the photopigment melanopsin (Gamlin et al., 2007; Markwell et al., 2010)

All experiments were conducted in the dark. Long and short wavelength stimuli were alternated to control for possible effects of melanopsin bistability on the pupil response (Mure et al., 2009) and fatigue (Feigl, Zele, et al., 2011; Kankipati et al., 2010). To account for age related, wavelength dependent attenuation by the optical media of the eye (Wooten, Hammond, Land, & Snodderly, 1999; Xu, Pokorny, & Smith, 1997), the retinal irradiances of the blue and red stimuli were estimated based on the optical density of the media (lens, cornea, aqueous and vitreous humours) for stimuli greater than 3° diameter (van de Kraats & van Norren, 2007). The estimated optical attenuation ranged between 0.28 and 0.35 log units for the blue light and was 0.15 log units for the red light across the age range of the participants (22–39 years old).

2.2.1 Experiment 1: Temporal properties of the tonic pupil response—Temporal summation was measured using a two-pulse paradigm (Baker, 1963; Ikeda, 1986; Zele, Cao, & Pokorny, 2008). Test stimuli were two 100 ms rectangular pulses separated by an inter-stimulus interval (ISI; 0, 64, 256, 512 or 1024 ms) and the control condition was a single 100 ms pulse. The stimulus duration was chosen to be as brief as possible to afford reliable discrimination between the short and long wavelength post-illumination pupil response (Park et al., 2011), while long enough for a high probability of photon capture by ipRGCs (Do et al., 2009) and within the critical duration for image and non-image forming functions (Alpern, McCready, & Barr, 1963; Webster, 1969). To determine that complete temporal integration was not limiting the summation for the 100 ms conditions, a control experiment was conducted with 16 ms pulse stimuli at high irradiance (conditions M^{+}_{BH}, M^{-}_{RH}; ISI: 0, 32, 64, 96, 128, 256, 512 ms and a single pulse). We hypothesised that melanopsin mediated temporal summation would present as an increase in the amplitude of the sustained post-illumination pupil response (condition M^{+}_{BH}), and non-melanopsin (outer retinal) mediated summation would present as an increase in the amplitude of the light evoked pupil constriction (conditions M^{-}_{RH}, M^{-}_{BL}, M^{-}_{RL}).

2.2.2 Experiment 2: Temporal properties of the phasic pupil response—The phasic response of the pupil light reflex was measured using five sinusoidal temporal modulation frequencies; 0.24 Hz (3 cycles) for 12.5 s, 0.50 Hz (6 cycles) for 12 s, 1.00 Hz (11 cycles) for 11 s, 1.98 Hz stimulus (20 cycles) for 10.10 s; and 4.08 Hz (41 cycles) for 10.05 s; and stimulus onset began at its minima (zero irradiance). Since ipRGCs are photon counters that signal absolute irradiance for long duration circadian processing, it was expected that melanopsin inputs to the pupil control pathway would show complete integration over the durations tested. The amplitude of the post-illumination pupil response would therefore be invariant as a function of stimulus temporal frequency because stimuli with different temporal frequencies had the same mean irradiance levels. If the integration period of the intrinsic ipRGC pathway was within the durations tested then the PIPR amplitude would be dependent upon photon temporal arrangement and vary systematically with stimulus temporal frequency. We hypothesised that melanopsin activation during the phasic pupil response (condition M^{+}_{BH}) would present as a decrease in the peak-trough amplitude, commensurate with melanopsin suppression of the PIPR amplitude. Impulse response functions were derived from the peak-trough amplitude data to determine the amplitude and timing of the phasic pupil response.

2.3 Participants

Fifteen participants (mean age = 28.3 years, *SD* = 5.9, range = 22 – 39; 8 males and 7 females) underwent a comprehensive ophthalmic examination including testing for afferent pupil defects, best-corrected visual acuity, intra ocular pressures with tonometry (Icare, Finland), slit lamp examination of the anterior eye, ophthalmoscopy and colour vision. All participants had normal eye health with a best-corrected visual acuity of 6/6 or greater. The right eye was dilated (Tropicamide 1% w/v, Bausch & Lomb) and reached maximal dilation before starting the test session (mean baseline fellow pupil diameter = 6.7 mm, *SD* = 0.67). Ten people participated in the 100 ms 2-pulse experiment (6 M^{+}_{BH}, M^{-}_{RH}; 4 M^{+}_{BL}, M^{-}_{RL}), four in the 16 ms 2-pulse control experiment (M^{+}_{BH}, M^{-}_{RH}) and seven in the phasic pupil response experiment (5 M^{+}_{BH}, M^{-}_{RH}; 2 M^{-}_{BL}, M^{-}_{RL}). Pilot testing was conducted for each of the conditions using one non-dilated participant; this data was found not to vary significantly from dilated and was thus included in the analyses. The University Human Research Ethics Committee approved the project and all experiments were conducted in accordance with the Code of Ethics of the World Medical Association (Declaration of Helsinki). Informed consent was obtained from all participants.

2.4 Procedure

After ophthalmic examination, Tropicamide 1% was applied to the participant's right eye and a 15 min dark adaptation period commenced during which the procedure was explained. Participants were aligned in the pupillometer in Maxwellian view. Head position was maintained with a supraorbital arch stabilizer, chinrest, temple bars and head restraint. A single pupil recording consisted of a 10 s pre-stimulus period in the dark, the stimulus light presentation as defined in the experimental conditions and a 40 s post-illumination period. A seven minute dark adaptation period was allowed between trials during which the participants removed their head from the pupillometer but remained seated. Two repeats were recorded for each stimulus for each participant, with a single session typically between

2 and 2.5 hours in duration. Repeats were conducted at a similar time of the day for each participant and all recordings were conducted in the morning or afternoon to prevent circadian dependent variability of ipRGC contributions to the pupil light reflex (Münch, Léon, Crippa, & Kawasaki, 2012; Zele et al., 2011).

2.5 Data Modelling, Pupil Metrics and Statistical Analyses

To account for individual differences in baseline pupil diameter (Pokorny & Smith, 1997), the data were normalised to the baseline diameter defined as the average during the five seconds immediately preceding stimulus onset. The maximum pupil constriction diameter and timing were analysed in Experiment 1. Maximum constriction timing was calculated from the first data point after stimulus onset which decreased in amplitude by at least 1% from the average of the three frames immediately preceding the 10s pre-stimulus time point. The PIPR was modelled with an exponential of the form $y = s * \exp(k * t) + r$ (Equation 1 where s, k and r were free parameters) (Feigl, Mattes, et al., 2011; Feigl, Zele, et al., 2011; Zele et al., 2011) by minimising sums of squared differences using the Solver analysis tool in Microsoft Excel (Microsoft Corporation). The melanopsin contribution to the PIPR was analysed at 6s post-stimulus offset (Park et al., 2011).

In Experiment 2, the phasic pupil response was calculated by extracting pupil peaks and troughs from the data using a peak detection function in Matlab (http://billauer.co.il/peakdet.html). Results were expressed as the phase (in degrees) of the average of the latencies of the identified pupil troughs (stimulus maximum irradiance) and peaks (stimulus minimum (zero) irradiance) for each stimulus frequency and wavelength. The initial pupil constriction at stimulus onset (i.e., during the first cycle) was discarded as it did not represent maximum pupil constriction as shown in subsequent constrictions. The peak-to-trough amplitudes for the 4.08 Hz condition were not large enough to allow reliable data extraction and so are not reported.

Impulse response functions (IRFs) (Ikeda, 1986) were derived from the temporal contrast sensitivity data using a Kramers-Kronig relation to reconstruct the temporal phase spectrum with a minimum phase assumption (Stork & Falk, 1987). Shinomori and Werner (2003) found the derived impulse response functions were similar with or without minimum phase assumption. Cao, Zele and Pokorny (2007) provide details of the procedures for deriving the IRFs, and discuss several caveats concerning the methodology.

Repeated measures ANOVAs [within: stimulus wavelength, inter-stimulus interval or frequency; between: irradiance level]) were conducted for 6s PIPR, maximum pupil constriction amplitude, peak-trough amplitude and phase. SPSS Statistics 19 (IBM) was used for statistical analysis.

3. Results

3.1 Experiment 1: Temporal properties of the tonic pupil response

Figure 1 shows the pupil light reflex as a function of 2-pulse interval from individual representative participants in response to the 4 conditions: M^{+}_{BH}, M^{-}_{RH}, M^{-}_{BL} and M^{-}_{RL} (panels A to D respectively). Figure 2 shows the group results for pupil constriction (timing,

A,B; diameter, C,D) and 6s PIPR (panel E,F). The panel insets in Figure 1B,C,D show the first 15 s after onset of the first pulse and highlight that two pupil constrictions become manifest with increasing 2-pulse interval for the low melanopsin excitation conditions, indicating a common temporal process. Pupil constriction amplitude is largest for the high melanopsin excitation condition M^{+}_{BH} compared to M^{-} conditions (Figure 1; 2C) and constriction amplitude increases with increasing ISI under all conditions [$F(5,40) = 25.575$, $p < .001$, $\eta^2_p = .762$; Figure 2C]. The time to maximum pupil constriction is slower (Figure 1A and inset) and decreases with increasing 2-pulse ISI for the condition with high melanopsin excitation (condition M^{+}_{BH}) compared to the conditions with low melanopsin excitation (Figure 1B,C,D and insets) which are stable from 0 ms to 512 ms, and then increase with 2-pulse ISI (Figure 2A). These differences implicate different temporal processing characteristics with high and low melanopsin excitations. The PIPR was more sustained with high melanopsin excitation (condition M^{+}_{BH}; Figure 2E, unfilled squares) than in the low melanopsin excitation conditions and the 6 s PIPR amplitude is independent of ISI for all melanopsin excitations [$F(5,40) = .722$, $p = .611$, $\eta^2_p = .083$; Figure 2E], suggesting that temporal summation does not depend upon ISI.

Group data for the high irradiance (M^{+}_{BH}, M^{-}_{RH}) 2-pulse 16 ms control experiment is shown in Figure 2B,D,F. As per the 100 ms data (Figure 2A), the blue 16 ms data (M^{+}_{BH}) exhibit a different pupil constriction time course to the red data (M^{-}_{RH}; Figure 2B), and the constriction amplitude increases as ISI increases for the red [$F(7, 21) = 16.375$, $p < .001$, $\eta^2_p = .845$] but not the blue condition [$F(7, 21) = .555$, $p < .784$, $\eta^2_p = .156$, Figure 2D). Bonferroni adjusted post-hoc t-tests revealed that the pupil constriction at 512 ms ISI was significantly larger than the control (single pulse), 0, 64, and 256 ms ISI constrictions for the red condition (asterisks in Figure 2D). The 6s PIPR amplitude did not change as a function of ISI [$F(7,21) = .516$, $p = .628$, $\eta^2_p = .147$, Figure 2F] for either M^{+}_{BH} or M^{-}_{RH} conditions [$F(7,21) = .777$, $p = .496$, $\eta^2_p = .206$].

3.2 Experiment 2: Temporal properties of the phasic pupil response

Figure 3 shows representative pupil recordings from an individual participant in response to conditions M^{+}_{BH}, M^{-}_{RH}, M^{-}_{BL} and M^{-}_{RL} (panels A to D respectively), with the insets depicting 15 s from light onset. The group data are shown in Figure 4. The 6s PIPR amplitude is independent of temporal frequency for high and low melanopsin excitations [$F(4,20) = .066$, $p = .991$, $\eta^2_p = .013$; Figure 4A], with the largest sustained PIPR amplitude with the high melanopsin excitation condition (M^{+}_{BH}). Pupil peak-trough amplitudes decreased with increasing frequency [$F(3,15) = 62.835$, $p < .001$, $\eta^2_p = .926$], with the interaction [wavelength*frequency*irradiance; $F(3,15) = 21.184$, $p < .001$, $\eta^2_p = .809$] indicating condition M^{+}_{BH} was significantly attenuated at all frequencies compared to the low melanopsin excitation conditions (Figure 4B). The phase of the pupil response decreased with increasing frequency [$F(3,15) = 89.015$, $p < .001$, $\eta^2_p = .947$; Figure 4C], with no phase differences between any stimulus wavelength or irradiance condition.

The impulse response functions derived from the phasic pupil data for each of the four conditions are monophasic, with similar time to peak amplitude ($M = 137$ ms, $SD = 6$; Figure 4D). The IRF amplitude was lowest for the high melanopsin excitation condition

M^{+}_{BH} consistent with its reduced peak-trough amplitude in Figure 4B. The IRF amplitudes were similar for the red low melanopsin excitation conditions (M^{-}_{RL} and M^{-}_{RH}), and largest for the low irradiance blue condition M^{-}_{BL}.

4. Discussion

This study investigated the temporal summation and temporal frequency response of the inferred melanopsin contributions to the human pupil light reflex. Experiment 1 demonstrated that the temporal summation properties of ipRGCs measured in the melanopsin mediated post-illumination pupil response were independent of 2-pulse interval (Figure 1; 2E), and that the amplitude and timing of the initial pupil constriction was different between the low melanopsin (inferred outer retina) and high melanopsin (inferred inner and outer retina) excitations such that condition M^{+}_{BH} was slower to reach maximum constriction amplitude and unable to resolve the successive light pulses (Figure 1; 2A,C). Experiment 2 demonstrated that the PIPR was independent of sinusoidal temporal frequency (Figure 3; 4A) and that the high melanopsin excitation condition attenuated the phasic peak-trough amplitude without altering phase (Figure 3; 4B,C).

Experiment 1 determined that the characteristics and time course of the pupil constriction show differences in temporal summation over 2-pulse interval for high and low melanopsin excitation. With high melanopsin excitation (M^{+}_{BH}), the timing of the pupil constriction was characterised by a broad minima (compare insets in Figure 1A to 1B,C,D) and a delay in time to maximum constriction (Figure 2A,B) compared to the low melanopsin excitation conditions which showed faster temporal responses. With 100 ms pulses the pupil constriction amplitude trended to increase as ISI increased (Figure 2C), indicating partial temporal summation occurs under all four melanopsin excitations. With 16ms low melanopsin excitation (M^{-}_{RH}) stimuli the constriction amplitude was largest at 512 ms, consistent with the summation trend observed by Baker (1963), however this pattern was not observed with the high melanopsin excitation condition (M^{+}_{BH}) (Figure 2D). We infer that the high and low melanopsin excitation conditions involve different processes: The slower process did not resolve two pulses in condition M^{+}_{BH} and functionally augments the timing (Figure 2A,B) and diameter (Figure 2C,D) of the minimum pupil constriction, consistent with melanopsin contributions to pupil constriction as identified in mouse models by Lucas et al. (2003). This time course is incompatible with the L-, M-, S-cone and rod excitation entailed by the M^{+}_{BH} stimulus (Table 1). McDougal and Gamlin (2010) show in humans that the spectral sensitivity derived from the half-maximal pupil constriction to short duration (1 s – 10 s), single pulse stimuli is dominated by outer retina signalling (consistent with the common response patterns found with the three low melanopsin excitations; Figure 2A), with melanopsin contributions present in the three-quarter maximal pupil constriction to 1.78 s pulses. Here, we identify a melanopsin input to the pupil that is initiated in response to briefly presented, 100 ms pulses that acts to slow the temporal response of the maximal pupil constriction.

The PIPR amplitude was invariant of the 2-pulse interval for both the 16 ms and 100 ms conditions (M^{+}_{BH}, M^{-}_{RH}, M^{-}_{BL}, M^{-}_{RL}; Figure 2E,F). That the stimulus irradiances did not saturate the PIPR suggests that complete summation of the melanopsin inputs to the PIPR

occurred with 2-pulse durations and intervals tested. We infer that the PIPR is dependent on the total number of photons above threshold and independent of their temporal arrangement. This is in contrast to the ISI-dependent summation evidenced by the M^- pupil constriction amplitudes (Figure 2C,D), which we infer are predominantly extrinsically signalled. Physiological recordings show that the latency to maximum intrinsic spiking response takes > 1.5 s (Berson et al., 2002; Dacey et al., 2005) and the intrinsic melanopsin driven response measured using the maximum 1024 ms 2-pulse interval (Figure 2E) is within this latency period, thus the PIPR exhibits complete summation over the time periods tested. For the extrinsic pathway activating conditions (M^-), physiological recordings show that the time to the first spike of an ipRGC after stimulus onset is faster for rods and cones than for the intrinsic response (Berson et al., 2002; Dacey et al., 2005), however based on the current findings, there are at least two possible interpretations for the locus of summation. It may be that summation occurs at a site presynaptic to ipRGCs. Alternatively, there is evidence in mice that multiple ipRGC subtypes project to the OPN (Chen, Badea, & Hattar, 2011) and this may hold for humans; the summation might therefore reflect the different temporal tuning characteristics of ipRGCs to intrinsic and extrinsic signals, allowing summation to occur within ipRGCs in the pupil control pathway. The locus of summation, in conjunction with how the intrinsic ipRGC signal is summed under ipsilateral versus contralateral stimulus presentations (to investigate summation in the midbrain) and the potential effect upon PIPR, are yet to be determined.

Experiment 2 determined that the amplitude of the ipRGC driven post-illumination pupil response was independent of input temporal frequency (Figure 3,4A). This observation is consistent with PIPR amplitude being dependent on the number of photons above threshold (Gamlin et al., 2007) and not the temporal distribution of light for the time intervals studied. The PIPR amplitude therefore displays characteristic photon counting properties as is observed in *in vitro* recordings of ipRGCs (Dacey et al., 2005; Wong, 2012) to signal environmental irradiance for photoentrainment (Panda et al., 2002). Temporal frequency response constancy suggests that the intrinsic melanopsin signal measured via the pupil control pathway does not have sufficient temporal resolution to discriminate between input frequencies, with phasic pupil modulation predominantly controlled by extrinsic photoreceptor inputs (Barrionuevo et al., 2014; Gooley et al., 2012). This is in agreement with the results of Experiment 1 which indicate low temporal resolution of the melanopsin mediated pupil responses.

The phasic pupil responses in Experiment 2 showed that the peak-trough amplitude of the melanopsin exciting condition M^+_{BH} was significantly lower than the M^- conditions. This indicates a signature interaction between melanopsin and outer retinal signalling can be observed in the pupil's phasic response. Comparison of the high irradiance red and blue conditions suggest that the intrinsic ipRGC signal suppresses the pupil's peak-trough amplitude by 41% and 51% respectively, although stimuli irradiance, luminance and wavelength are also factors. The phasic pupil responses revealed low-pass peak-trough amplitudes for all conditions (Figure 4C) with phase lag increasing with increasing frequency (means: 0.24 Hz = −47.84°; 1.98 Hz = −335.12°) and a critical flicker frequency approaching 4 Hz (Figure 4B). These phase estimates are similar to past reports of the

dynamic response of the pupil to sinusoidal stimulation (Clarke et al., 2003; Stark, 1962; Stark & Sherman, 1957), but which did not explicitly study ipRGC function. Clark et al. (2003) for example, used a dim (scotopic) adapting background that was similar to the dark background in this study but the stimulus light was not optimised for melanopsin excitation. In comparison, a recent study using silent substitution to measure rod, cone and melanopsin photoreceptor inputs to the pupil control pathway with 1 Hz stimuli under steady state light adapted conditions found the phase delay decreased as the adapting light level shifted from mesopic to photopic illuminations (Barrionuevo et al., 2014). The role of the contribution of methodological differences to the phase estimates, including the effect of the dark and light adapted conditions, stimulus contrast and intrinsic noise in the pupillary pathways still need to be explored.

Impulse response functions derived to quantify the phasic temporal response of the pupil light reflex (Figure 4D) are monophasic and exhibit consistent time-to-peaks (M =136.5 ms, SD = 6.25) across the melanopsin and non-melanopsin activating conditions. This time-to-peak amplitude is more than 60–80 ms slower than the longest estimates for rods and cones as derived for human reaction time, 2-pulse and temporal contrast sensitivity measurements (see Cao, Zele & Pokorny, 2007), and will contain an additional latency inherent to the PLR pathway including the iris musculature (Loewenfeld, 1993). That the IRF amplitude was lower for melanopsin activating conditions than the outer retina activating conditions is consistent with the proposal that the intrinsic ipRGC contribution to the pupil constriction acts to reduce the peak to trough amplitude (Figure 4B), but without introducing a delay in the time to peak (Figure 4C). This suggests an interaction between two different signal generators; extrinsic outer retina photoreceptor signals which mediate the low pass temporal frequency response (Gooley et al., 2012) and the intrinsic (melanopsin) inner retina ipRGC signals which attenuate the magnitude of the pupil's response irrespective of flicker frequency. Based on the results of this study, we infer that the similar temporal frequency amplitude and phase response for the three low melanopsin excitation conditions; low irradiance blue (M^{-}_{BL}) and red (M^{-}_{RL}) stimuli (Figure 4B,C blue and red filled symbols) and the high irradiance red (M^{-}_{RH}) stimuli (Figure 4B,C red unfilled symbols); measured under dark adapted conditions indicate a common mechanism mediates pupillary dynamics in the three conditions. With further refinement, the sinusoidal paradigm may find clinical applications in the assessment of inner and outer retinal function. The high melanopsin excitation condition reflects contributions from all three photoreceptor types, offering an opportunity to study inner and outer retinal photoreceptor interactions as well as the efferent pathways which give rise to the pupil light reflex (Feigl & Zele, 2014).

As shown in Table 1, it is difficult to excite melanopsin using single narrow-band stimuli without also exciting rods and S-cones. However, the temporal properties exhibited under condition M+ are distinct from outer retinal mechanisms and are best explained as melanopsin inputs to the pupil control pathway. The PIPR is mediated by the intrinsic melanopsin signal as its spectral sensitivity matches that of the melanopsin nomogram (Feigl & Zele, 2014; Gamlin et al., 2007; Markwell et al., 2010), although this has yet to be shown for the 6 s PIPR metric. The minimum pupil diameter metrics quantified under the M^{+} condition only were found to have slower temporal dynamics, a longer latency to minimum

pupil diameter and more variability compared to those quantified under the M^- conditions (which are expected to be dominated by rod and/or cone signaling) for both the 100 ms and 16 ms stimuli (Figure 2A–D); despite the ratio of photoreceptor excitations not differing between low and high irradiance conditions (Table 1). The mean phasic pupil diameter is also smallest for the high irradiance blue condition (M^+) even though the quantal flux is the same for the high irradiance red condition (M^-) This finding is consistent with data from mice, that melanopsin activation is required to achieve maximum constriction at high irradiances (Lucas et al., 2003).

5. Conclusions

We provide the initial observation that the pupil control pathway displays complete temporal summation in the PIPR to short duration (100 ms) stimuli. The melanopsin mediated PIPR amplitude is independent of the inter-stimulus interval between two light pulses up to 1024 ms, and independent of the temporal frequency of sinusoidal stimuli (0.24 Hz to 4.08 Hz). The maximum pupil constriction amplitude to short 2-pulse stimuli demonstrates contributions from both the inner and outer retina: Melanopsin activating stimuli (M^+_{BH}) display lower temporal resolution, reflecting the slower temporal properties of the melanopsin pathway. This manifests as a delay in the time to maximum pupil constriction and an inability of the pupil to resolve successive light pulses. For outer retinal photoreceptor signals transmitted extrinsically via ipRGCs to the pupil control pathway, summation likely occurs at a locus presynaptic to ipRGCs, or may result from different tuning characteristics of the multiple ipRGC subtypes. We observe a signature interaction between melanopsin and outer retinal signalling in the pupil's phasic response, with melanopsin excitation significantly attenuating the peak-trough amplitude without altering phase.

Acknowledgments

Australian Research Council Discovery Projects DP140100333 (AJZ and BF), NEI R01EY019651 (DC), and a UIC core grant for vision research P30-EY01792 supported this research.

References

Alpern M, McCready DW, Barr L. The dependence of the photopupil response on flash duration and intensity. The Journal of General Physiology. 1963; 47(2):265–278. [PubMed: 14080815]

Baker FH. Pupillary response to double-pulse stimulation; a study of nonlinearity in the human pupil system. Journal of the Optical Society of America. 1963; 53(12):1430–1436. [PubMed: 14134099]

Barrionuevo PA, Nicandro N, McAnany JJ, Zele AJ, Gamlin P, Cao D. Assessing rod, cone and melanopsin contributions to human pupil flicker responses. Investigative Ophthalmology & Visual Science. 2014; 55(2):719–727. [PubMed: 24408974]

Beer RD, MacLeod DIA, Miller TP. The extended maxwellian view (BIGMAX): A high-intensity, high-saturation color display for clinical diagnosis and vision research. Behavior Research Methods. 2005; 37(3):513–521. [PubMed: 16405148]

Berson DM, Dunn FA, Takao M. Phototransduction by retinal ganglion cells that set the circadian clock. Science. 2002; 295:1070–1073. [PubMed: 11834835]

Cao D, Zele AJ, Pokorny J. Linking impulse response functions to reaction time: Rod and cone reaction time data and a computational model. Vision Research. 2007; 47(8):1060–1074. [PubMed: 17346763]

Chen SK, Badea TC, Hattar S. Photoentrainment and pupillary light reflex are mediated by distinct populations of ipRGCs. Nature. 2011; 476(7358):92–95. [PubMed: 21765429]

Clarke RJ, Zhang H, Gamlin PDR. Characteristics of the pupillary light reflex in the alert rhesus monkey. Journal of Neurophysiology. 2003; 89(6):3179–3189. [PubMed: 12611973]

Dacey DM, Gamlin PD, Liao HW, Peterson BB, Pokorny J, Robinson FR, Smith VC, Yau KW. Melanopsin-expressing ganglion cells in primate retina signal colour and irradiance and project to the LGN. Nature. 2005; 433(7027):749–754. [PubMed: 15716953]

Do MTH, Kang SH, Xue T, Zhong H, Liao HW, Bergles DE, Yau KW. Photon capture and signalling by melanopsin retinal ganglion cells. Nature. 2009; 457(7227):281–287. [PubMed: 19118382]

Do MTH, Yau KW. Intrinsically photosensitive retinal ganglion cells. Physiological Reviews. 2010; 90(4):1547–1581. [PubMed: 20959623]

Feigl B, Mattes D, Thomas R, Zele AJ. Intrinsically photosensitive (melanopsin) retinal ganglion cell function in glaucoma. Investigative Ophthalmology & Visual Science. 2011; 52(7):4362–4367.10.1167/iovs.10-7069 [PubMed: 21498620]

Feigl B, Zele AJ. Melanopsin-expressing intrinsically photosensitive retinal ganglion cells in retinal disease. Optometry and Vision Science. 2014; 91(8):894–903. [PubMed: 24879087]

Feigl B, Zele AJ, Fader SM, Howes AN, Hughes CE, Jones KA, Jones R. The post-illumination pupil response of melanopsin-expressing intrinsically photosensitive retinal ganglion cells in diabetes. Acta Ophthalmologica. 2011; 90(3):e230–e234. [PubMed: 21883986]

Gamlin PDR, McDougal DH, Pokorny J, Smith VC, Yau KW, Dacey DM. Human and macaque pupil responses driven by melanopsin-containing retinal ganglion cells. Vision Research. 2007; 47(7):946–954. [PubMed: 17320141]

Gooley JJ, Ho Mien I, St Hilaire MA, Yeo SC, Chua EC, van Reen E, Hanley CJ, Hull JT, Czeisler CA, Lockley SW. Melanopsin and rod–cone photoreceptors play different roles in mediating pupillary light responses during exposure to continuous light in humans. The Journal of Neuroscience. 2012; 32(41):14242–14253. [PubMed: 23055493]

Gooley JJ, Lu J, Fischer D, Saper CB. A broad role for melanopsin in nonvisual photoreception. The Journal of Neuroscience. 2003; 23(18):7093–7106. [PubMed: 12904470]

Güler AD, Ecker JL, Lall GS, Haq S, Altimus CM, Liao HW, Barnard AR, Cahill H, Badea TC, Zhao H. Melanopsin cells are the principal conduits for rod–cone input to non-image-forming vision. Nature. 2008; 453(7191):102–105. [PubMed: 18432195]

Hattar S, Kumar M, Park A, Tong P, Tung J, Yau KW, Berson DM. Central projections of melanopsin-expressing retinal ganglion cells in the mouse. Journal of Comparative Neurology. 2006; 497(3):326–349. [PubMed: 16736474]

Hattar S, Liao HW, Takao M, Berson DM, Yau KW. Melanopsin-containing retinal ganglion cells: Architecture, projections, and intrinsic photosensitivity. Science. 2002; 295(5557):1065–1070. [PubMed: 11834834]

Ikeda M. Temporal impulse response. Vision Research. 1986; 26(9):1431–1440. [PubMed: 3303667]

Kankipati L, Girkin CA, Gamlin PD. Post-illumination pupil response in subjects without ocular disease. Investigative Ophthalmology & Visual Science. 2010; 51(5):2764–2769.10.1167/iovs.09-4717 [PubMed: 20007832]

Loewenfeld, IE. The Pupil. Anatomy, physiology, and clinical applications. Vol. 1. Ames, Iowa: Iowa State University Press; 1993.

Lucas RJ, Douglas R, Foster R. Characterization of an ocular photopigment capable of driving pupillary constriction in mice. Nature Neuroscience. 2001; 4(6):621–626.

Lucas RJ, Hattar S, Takao M, Berson D, Foster R, Yau KW. Diminished pupillary light reflex at high irradiances in melanopsin-knockout mice. Science. 2003; 299(5604):245–247. [PubMed: 12522249]

Lucas RJ, Peirson SN, Berson DM, Brown TM, Cooper HM, Czeisler CA, Figueiro MG, Gamlin PD, Lockley SW, O'Hagan JB, Price LLA, Provencio I, Skene DJ, Brainard GC. Measuring and using light in the melanopsin age. TRENDS in Neurosciences. 2014; 37(1):1–9. http://dx.doi.org/10.1016/j.tins.2013.10.004. [PubMed: 24287308]

Markwell EL, Feigl B, Zele AJ. Intrinsically photosensitive melanopsin retinal ganglion cell contributions to the pupillary light reflex and circadian rhythm. Clinical and Experimental Optometry. 2010; 93(3):137–149. [PubMed: 20557555]

McDougal DH, Gamlin PD. The influence of intrinsically-photosensitive retinal ganglion cells on the spectral sensitivity and response dynamics of the human pupillary light reflex. Vision Research. 2010; 50(1):72–87. [PubMed: 19850061]

McDougal, DH.; Gamlin, PDR. Pupillary control pathways. In: Masland, RH.; Albright, TD.; Albright, TD.; Masland, RH.; Dallos, P.; Oertel, D.; Firestein, S.; Beauchamp, GK.; Bushnell, MC.; Basbaum, AI.; Kaas, JH.; Gardner, EP., editors. The Senses: A Comprehensive Reference. New York: Academic Press; 2008. p. 521-536.

Münch M, Léon L, Crippa SV, Kawasaki A. Circadian and wake-dependent effects on the pupil light reflex in response to narrow-bandwidth light pulses. Investigative Ophthalmology & Visual Science. 2012; 53(8):4546–4555.10.1167/iovs.12-9494 [PubMed: 22669721]

Mure LS, Cornut PL, Rieux C, Drouyer E, Denis P, Gronfier C, Cooper HM. Melanopsin bistability: A fly's eye technology in the human retina. PLoS ONE. 2009; 4(6):e5991.10.1371/journal.pone.0005991 [PubMed: 19551136]

Panda S, Sato TK, Castrucci AM, Rollag MD, DeGrip WJ, Hogenesch JB, Provencio I, Kay SA. Melanopsin (Opn4) requirement for normal light-induced circadian phase shifting. Science. 2002; 298(5601):2213. [PubMed: 12481141]

Park JC, Moura AL, Raza AS, Rhee DW, Kardon RH, Hood DC. Toward a clinical protocol for assessing rod, cone, and melanopsin contributions to the human pupil response. Investigative Ophthalmology & Visual Science. 2011; 52(9):6624–6635.10.1167/iovs.11-7586 [PubMed: 21743008]

Pokorny J, Smith V. How much light reaches the retina? Documenta Ophthalmologica Proceedings Series. 1997; 59:491–512.

Provencio I, Rollag MD, Castrucci AM. Photoreceptive net in the mammalian retina. Nature. 2002; 415(6871):493–493. [PubMed: 11823848]

Schmidt TM, Kofuji P. Differential cone pathway influence on intrinsically photosensitive retinal ganglion cell subtypes. The Journal of Neuroscience. 2010; 30(48):16262–16271. [PubMed: 21123572]

Shinomori K, Werner JS. Senescence of the temporal impulse response to a luminous pulse. Vision Research. 2003; 43(6):617–627. [PubMed: 12604098]

Stark L. Biological rhythms, noise, and asymmetry in the pupil-retinal control system. Annals of the New York Academy of Sciences. 1962; 98(4):1096–1108. [PubMed: 13983452]

Stark L, Baker F. Stability and oscillations in a neurological servomechanism. Journal of Neurophysiology. 1959; 22(2):156–164. [PubMed: 13642092]

Stark L, Sherman PM. A servoanalytic study of consensual pupil reflex to light. Journal of Neurophysiology. 1957; 20:17–26. [PubMed: 13398849]

Stork DG, Falk DS. Temporal impulse responses from flicker sensitivities. Journal of the Optical Society of America, A. 1987; 4(6):1130–1135.

Tsujimura S, Ukai K, Ohama D, Nuruki A, Yunokuchi K. Contribution of human melanopsin retinal ganglion cells to steady-state pupil responses. Proceedings of the Royal Society B: Biological Sciences. 2010; 277(1693):2485–2492.

van de Kraats J, van Norren D. Optical density of the aging human ocular media in the visible and the UV. Journal of the Optical Society of America, A. 2007; 24(7):1842–1857.

Webster JG. Critical duration for the pupillary light reflex. Journal of the Optical Society of America. 1969; 59(11):1473–1478. [PubMed: 5349098]

Wong KY. A retinal ganglion cell that can signal irradiance continuously for 10 hours. The Journal of Neuroscience. 2012; 32(33):11478–11485. [PubMed: 22895730]

Wooten BR, Hammond BR, Land RI, Snodderly DM. A practical method for measuring macular pigment optical density. Investigative Ophthalmology & Visual Science. 1999; 40(11):2481–2489. [PubMed: 10509640]

Xu J, Pokorny J, Smith VC. Optical density of the human lens. Journal of the Optical Society of America, A. 1997; 14(5):953–960.

Zele AJ, Cao D, Pokorny J. Rod-cone interactions and the temporal impulse response of the cone pathway. Vision Research. 2008; 48(26):2593–2598. [PubMed: 18486960]

Zele AJ, Feigl B, Smith SS, Markwell EL. The circadian response of intrinsically photosensitive retinal ganglion cells. PloS ONE. 2011; 6(3):e17860.10.1371/journal.pone.0017860 [PubMed: 21423755]

Highlights

- Post Illumination Pupil Response amplitude displays complete temporal summation.
- PIPR amplitude is independent of stimulus temporal frequency.
- Melanopsin activation attenuates peak-trough amplitudes of the phasic pupil response.

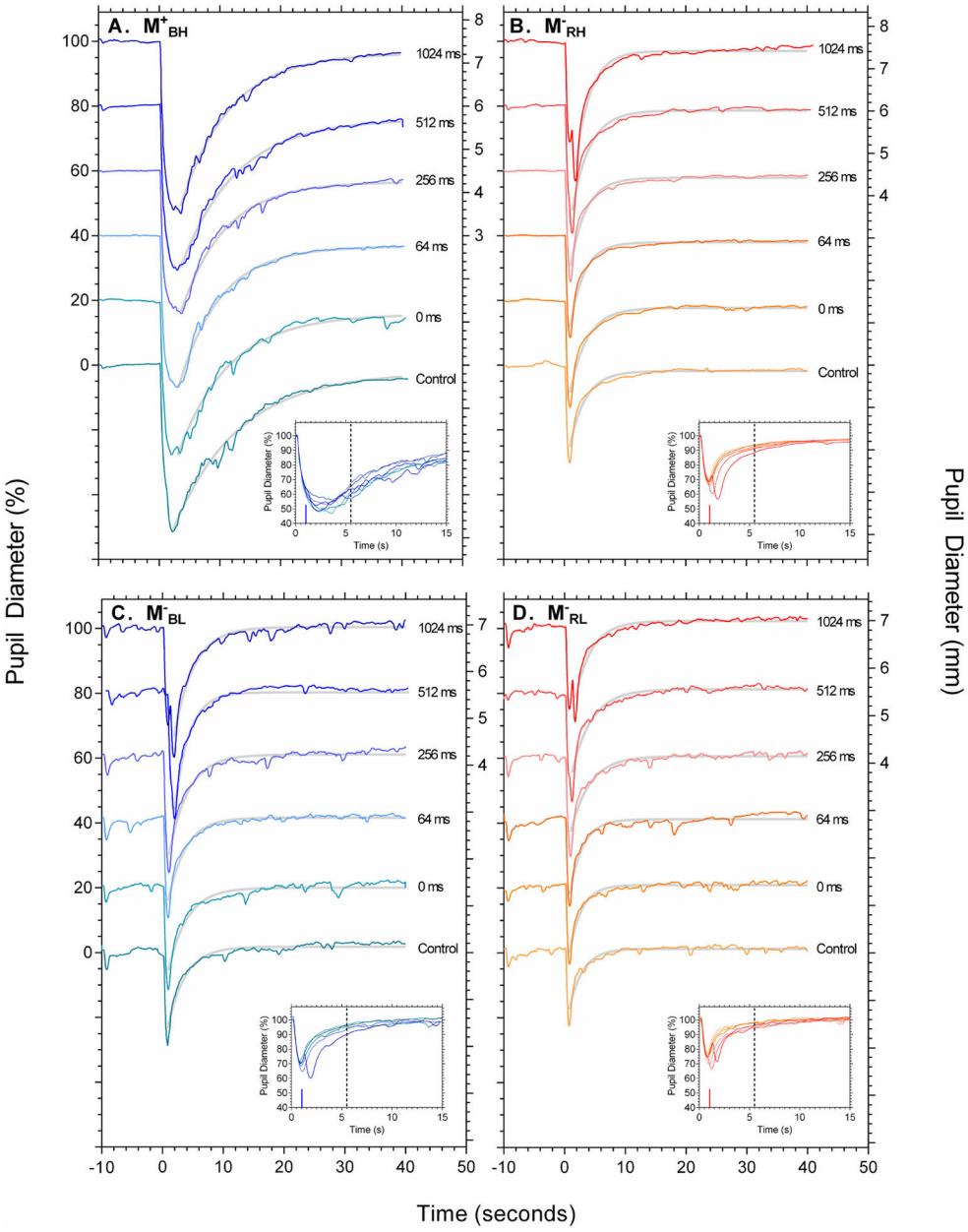

Figure 1.

Representative 100ms 2-pulse pupil responses for conditions M^{+}_{BH}, M^{-}_{RH}, M^{-}_{RL}, and M^{-}_{BL} (clockwise from top left). In each panel the data are vertically offset by 20% as a function of the 2-pulse inter-stimulus interval. Pupil diameter is expressed as percentage baseline on the left axis, and millimetres for the 1024ms condition only on the right axis. The control condition shows the pupillary response to the single 100 ms pulse. The insets show the first 15 seconds of the pupillary trace after stimulus onset. The vertical line indicates the timing of the second pulse of the longest ISI condition (1024 ms). The dashed vertical line denotes the timing of the 6 s PIPR. The grey lines are the best fitting

exponential functions (Equation 1) used to derive the 6 s PIPR. The data in each panel are for a single observer.

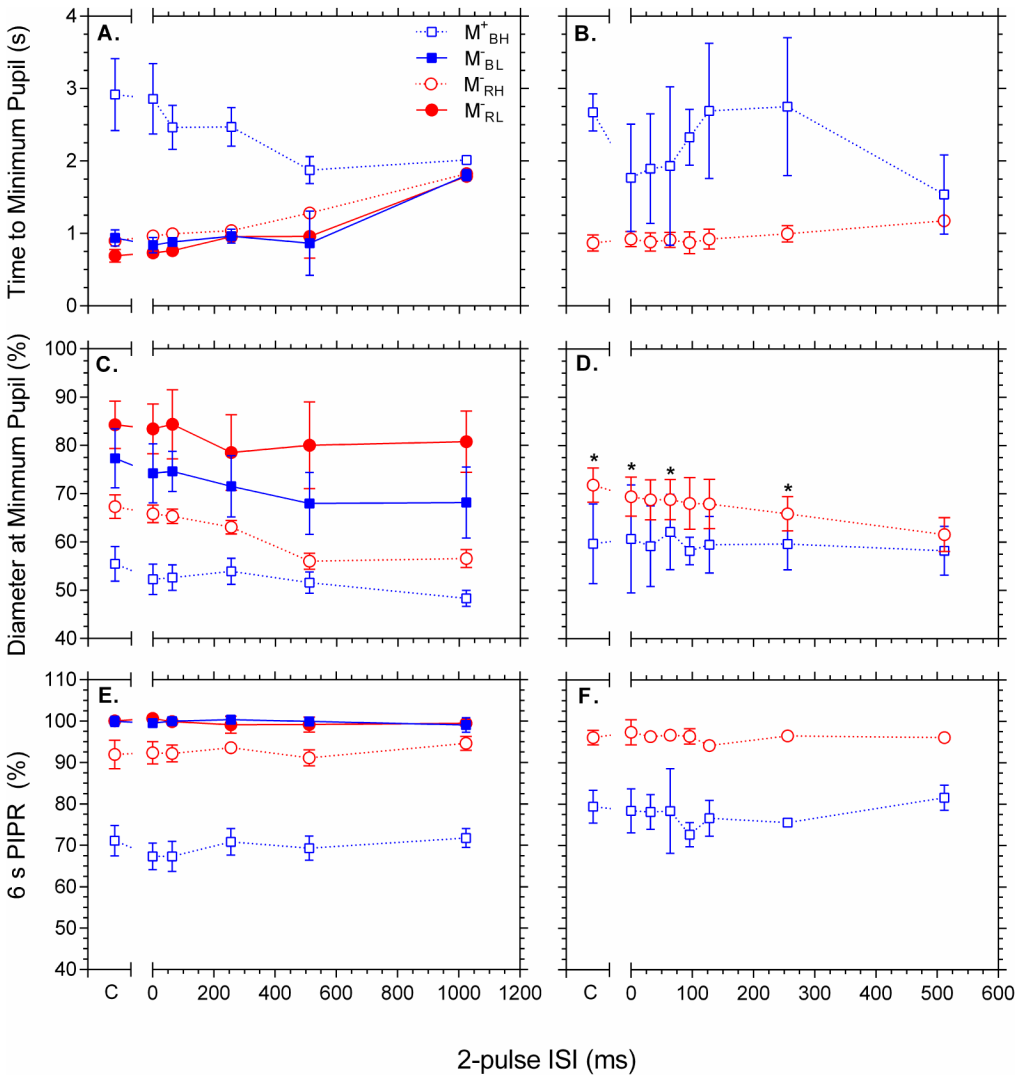

Figure 2.

Average 100ms (panels A,C,E) and 16ms (panels B,D,F) 2-pulse normalised minimum pupil timing and diameter, and 6s PIPR as a function of ISI. Panels 2A,B show the time at which maximum constriction is reached and Panels 2C,D show the diameter of this constriction. Panels 2E,F show the 6 s PIPR. Asterisks in panel 2D denote a significant difference from 512 ms data point (Bonferroni adjusted pairwise comparisons, familywise $p = .05$). Conditions are coded: M^{+}_{BH}, open blue squares; M^{-}_{RH}, open red circles; M^{-}_{RL}, filled red circles and M^{-}_{BL}, filled blue circles.

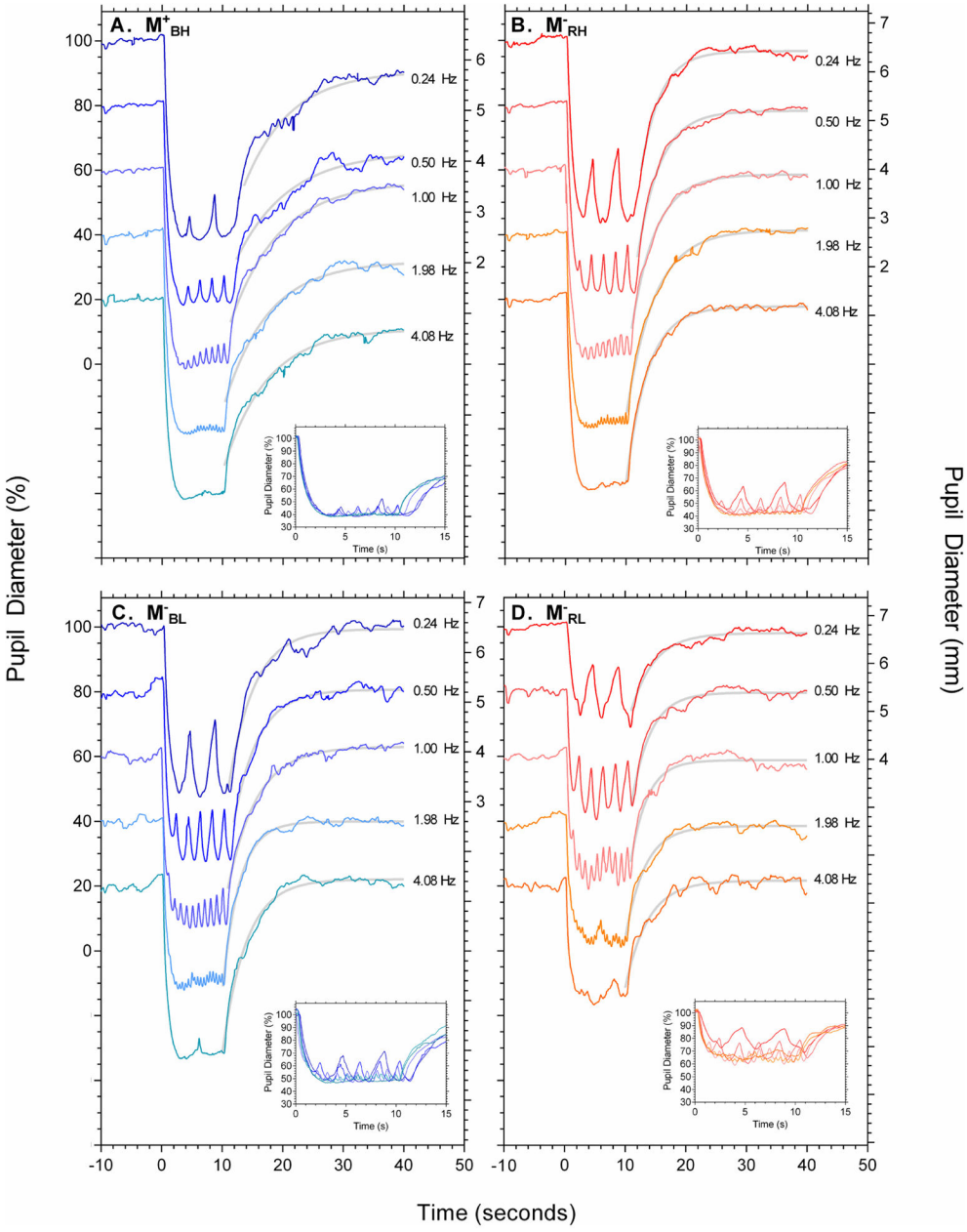

Figure 3.

Representative sinusoidal pupil responses for conditions M^{+}_{BH}, M^{-}_{RH}, M^{-}_{RL}, and M^{-}_{BL} (clockwise from top left). In each panel the data are vertically offset by 20% as a function of stimulus frequency. Pupil diameter is expressed as percentage baseline on the left axis, and millimetres for the 0.24 Hz condition only on the right axis. The insets show the first 15 seconds of the pupillary trace after stimulus onset. The grey lines are the best fitting exponential functions (Equation 1) used to derive the 6 s PIPR. The data in each panel are for a single observer.

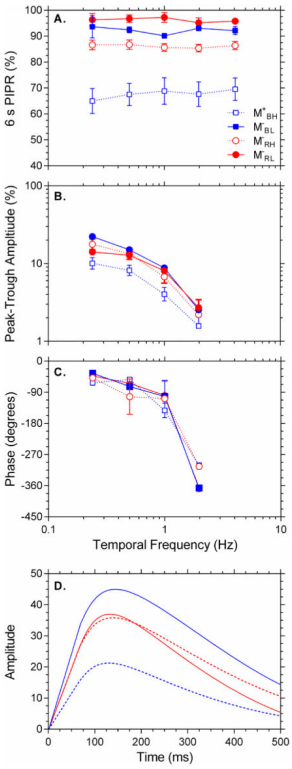

Figure 4.

Average sinusoidal data depicting 6s PIPR, peak-trough amplitude, phase and Impulse Response Function. Panel 4A shows the 6 s PIPR as a function of stimulus frequency. Panel 4B shows the peak-trough amplitude and Panel 4C the phase lag in degrees between the input stimulus and the pupil's measured response. Panel 4D shows the derived Impulse Response Function for frequencies 0.24 to 1.98 Hz. Conditions are coded: M^{+}_{BH}, dashed blue line; M^{-}_{RH}, dashed red line; M^{-}_{RL}, solid red line and M^{-}_{BL}, solid blue line.

Table 1

Estimated photoreceptor excitations (α-opic lux) for each stimulus condition

	α-opic lux				
Stimulus	**Melanopic (Melanopsin)**	**Rhodopic (Rod)**	**Cyanopic (S-cone)**	**Chloropic (M-cone)**	**Erythropic (L-cone)**
M^{+}_{BH} (464 nm, 15.2 log photons.cm^{-2}.s^{-1})	4453	3103	5333	1502	767
M^{-}_{RH} (638 nm, 15.2 log photons.cm^{-2}.s^{-1})	2.78	15.76	1.85	256	1036
M^{-}_{BL} (464 nm, 11.4 log photons.cm^{-2}.s^{-1})	0.71	0.49	0.85	0.24	0.12
M^{-}_{RL} (638 nm, 11.4 log photons.cm^{-2}.s^{-1})	4.41×10^{-4}	2.5×10^{-3}	2.93×10^{-4}	4.05×10^{-4}	0.16